Towards a Realistic Performance Analysis of Storage Systems in Smart Grids

Y. Ghiassi-Farrokhfal, S. Keshav
Computer Science Dept.

C. Rosenberg
Electrical & Computer Eng. Dept.

University of Waterloo

Technical Report CS-2013-18

Abstract

Energy storage devices (ESDs) such as lithium-ion batteries and flywheels have the potential to revolutionize the electricity grid by allowing the smoothing of variable-energy generator output, and the time-shifting of demand away from peak times. Numerous recent investigations have studied the impact of ESDs on energy systems, but usually by assuming ideal ESD behaviour, such as infinite ESD charging and discharging rates, and zero self-discharge. However, real-life ESDs are far from ideal. We investigate the effect of non-ideal ESD behaviour on system performance, presenting an analytical ESD model that retains much of the simplicity of an ideal ESD, yet captures many (though not all) non-ideal behaviours. This allows us to compute performance bounds for systems using non-ideal ESDs using standard teletraffic techniques. We provide performance results for five widely used ESD technologies and show that our models can closely approximate numerically computed performance bounds.

I. Introduction

Both electricity generation from renewable energy sources and electricity demand are stochastic processes. This makes them difficult to manage and control. Energy storage devices (ESDs) can smooth out variations in generation and demand, greatly simplifying grid operation. Therefore, there has been a considerable amount of work in the design of many types of ESD-based systems (see Fig. 1). Examples are off-grid networks which use renewable energy to serve their

This work was done at the David R. Cheriton School of Computer Science and ECE Dept., University of Waterloo.

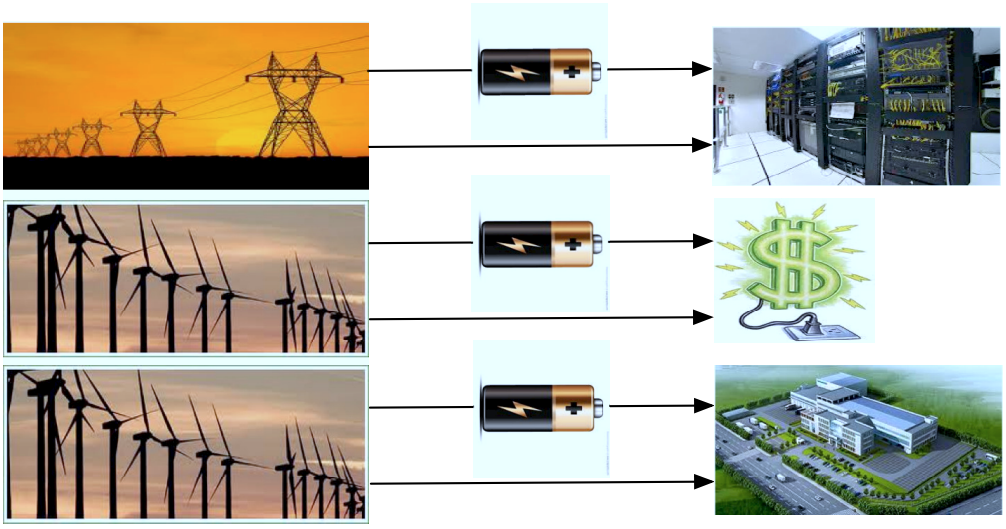

Fig. 1: Some of the ESD applications in energy systems (top to bottom): load shifting of data centres, renewable energy in electricity market, and renewable energy in off-grid networks.

demands (stochastic energy source, stochastic demand) [13], load shaping in on-grid networks (deterministic energy source, stochastic demand) [21], and firming renewable energy sources for electricity market (stochastic energy source, deterministic demand) [6].

The traditional approach to design an ESD-based energy system is numerical simulation, as in [8], [19], [24]. Simulation methods are used to compute either active power [19], or current-voltage (I-V) values [8]. I-V simulation contains more information than active power simulation about energy system operation, as it allows the monitoring of both current and voltage. However, I-V simulation is more complex, because ESDs must be modelled by (complex) electric circuits [14], [20] there are sensitive to the choice of ESD technology [18].

Although quite precise, design based on simulation is feasible only when large datasets are available to allow computation of tail bounds for small target failure probabilities. Moreover, the simulation must be repeated to study the sensitivity to any single parameter, which is computationally expensive.

As an alternative to simulation, and inspired by the analogy between storing energy in an ESD and traffic buffering in a packet network, several recent papers have adopted the analytical techniques developed for teletraffic analysis to study generic ESD-based energy systems. Examples include computing the loss of power probability in a distribution network [3], using non-

asymptotic Kesidis bounds for regulated traffic [4], and using a network calculus framework [22], [23].

Arguably, the technique that is best suited for the analysis of ESD-based energy systems is the network calculus approach [5], [7], [15] because it precisely matches the characteristics of a smart grid system, that is, non-asymptotic, non-stationary, and fluid flow. Unfortunately, the elegant mapping between teletraffic networks and smart grids makes the strong assumption of an ideal ESD, that is, one that looks like a RAM network buffer. In this paper, we show that this mapping does *not* hold for non-ideal ESDs, *bringing into question the validity of existing results*. The take-away message from our paper is that it is critical to model non-ideal ESD behaviour and, in fact, our approach does this very well. Specifically:

1) We provide a simple and general model that permits the performance analysis of energy systems using non-ideal ESDs based on *any* underlying technology.
2) We use our model to compute analytical bounds on loss of power and waste of power and show that our analytical performance bounds closely approximate numerical simulations.
3) We demonstrate that the choice of ESD technology as well as its non-ideal behaviour both significantly impact the performance of an energy system.

The remainder of the paper is organized as follows. In Section II, we review some of the most widely used ESD technologies along with their characteristics. We present the system model in Section III. We show in Section IV how to convert a complex non-ideal ESD model to an ideal one. In Section V, we employ network calculus to derive performance bounds using our model. In Section VI, we show the importance of accounting for non-ideal ESD behaviour, evaluate our bounds, and compare the performance of different storage technologies. Finally, we conclude our paper in Section VII.

II. Background on storage systems

Four ESD technologies are in common use today: mechanical, thermo-dynamic, electrochemical, and electro-magnetic, each with its own characteristics. These include:

• **ESD size (B (Wh)):** This is the maximum amount of energy that can be stored in an ESD. Some ESD technologies require devices to have a maximum or minimum size. ESD size decreases over long time intervals due to deteriorations. This must be accounted for, when analyzing an ESD over a large time, e.g., in a lifetime maximization problem [9]. However,

Name	*Description (units)*
T_u	Time unit (hour)
$S(t)(S'(t))$	Input power (virtual input power) at time t (W)
$D(t)(D'(t))$	Demand power (virtual demand power) at time t (W)
$\overline{\mathcal{S}}(\underline{\mathcal{S}})$	Upper (lower) envelope on the input power (W)
$\overline{\mathcal{D}}(\underline{\mathcal{D}})$	Upper (lower) envelope on the demand power (W)
B	ESD size (Wh)
$\alpha_c(\alpha_d)$	ESD charging (discharging) power limit (W)
η	ESD efficiency
γ	ESD leakage power rate (W)
DoD	ESD depth of discharge
$l(t)$	Loss of power at time t (W)
$w(t)$	Waste of power at time t (W)

TABLE I: Notations used in this paper

	Lead-acid	Lithium-ion	Scaps	FW	CAES
Efficiency	0.75	0.85	0.95	0.95	0.68
Charge time (=ESD size/Charge rate)	8-16h	2-4h	1-10 sec	30sec-3min	15 min
Discharge rate to charge rate ratio	10	5	1	1	4
Self-discharge/ day (=self-discharge rate $\times$ day / ESD size) (%)	0.3	0.1	20	100	0
DoD	0.80	0.80	1	1	1

TABLE II: ESD characteristics [1], [21]

ESD size can be assumed to be fixed, if short-term performance metrics are analyzed (such as in this paper).

• **Specific energy (or power) (Wh/m^3 or Wh/kg (W/m^3 or W/kg)):** This is the energy (or power) provided per unit volume or per unit mass.

• **Energy (power) cost ($/Wh ($/W)):** This is the monetary cost to provide a unit of energy (power).

• **Storage charging and discharging rate limit (α_c and α_d (W)):** This is the limit on the charge or discharge power. Typical discharge rates are many times greater ($10\times$ for lead-acid and $5\times$ for lithium-ion batteries) than the charging rate.

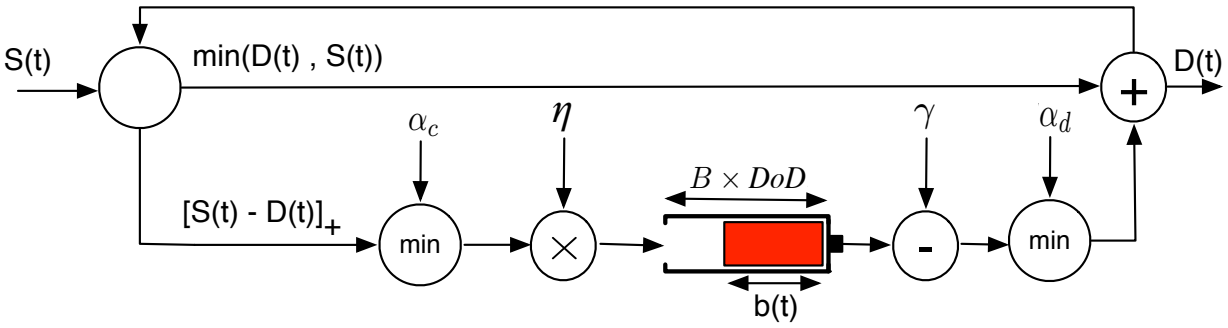

Fig. 2: A stochastic power source S equipped with an ESD to serve a demand power D. The physical constraints of the ESD are α_c, α_d, η, γ, and DoD. Note: $[x]_+ = \max\{0, x\}$ for any x.

• **ESD efficiency** ($0 \leq \eta \leq 1$)**:** Due to inherent inefficiencies, each unit of energy stored is reduced to η units that can be used at a later time. ESDs converting electrical energy to other forms typically have lower efficiencies.

• **Self-discharge** (γ **(W)):** Stored energy leaks over time at the rate γ. Large self-discharge rates become problematic when ESDs need to store large amounts of energy for a long period of time.

• **Depth-of-discharge** ($0 \leq$ **DoD** ≤ 1)**:** While the entire capacity of some ESDs can be used for energy storage, battery life is extended if only a fraction (DoD) of available capacity is used. There is extensive work to determine the relationship between battery lifetime and DoD, e.g., [17].

• **Temperature-dependency:** Operating temperature can affect the charging and discharging rates and the lifetime of a battery. The operation of other ESDs, however, is nearly independent of the temperature. Despite the importance of this factor, it is not yet known how temperature can impact the performance of a battery. Thus, we do not consider it in our model, assuming that the dynamics of the impacts of temperature change on the physical constraints of the battery is slower than the dynamics of the battery charging/discharging.

This work evaluates the following five representative ESD technologies:

1) *Lead-acid battery* (electrochemical): This is a widely-used battery because of its low energy cost, high specific power, simple manufacturing, and its lowest self-discharge rate among all batteries. It has, however, a small charging rate, a low specific energy, and a limited life cycle.

2) *Lithium-ion battery* (electrochemical): This type of battery has a high energy density, a high energy efficiency, and a low discharge rate. One of the main disadvantages of this battery is its price, which can be $3\times$ larger than a lead-acid battery.
3) *Supercapacitor (Scap)* (electro-magnetic): Supercapacitors store energy by means of static charges and consist of two conducting plates, which are separated by a superconductor. Scaps have large life cycles, high power densities, large charging rates, and no constraints on DoD. Scaps, however, have low energy densities, high self-discharge rates, and large power costs.
4) *Flywheel (FW)* (mechanical): This type of storage uses the moments of rotating wheels or cylinders to store and generate electricity. Flywheels have high power densities, large cycle lives, high efficiencies, no DoD restriction, but large energy costs.
5) *Compressed air energy storage (CAES)* (thermo-dynamic): This device stores energy in the form of compressed air in a room and releases it to rotate a turbine for electricity generation. CAES has low energy cost, but high power cost. It also has low energy and low power density. It has small efficiency, but no restriction on DoD.

Due to the diversity of ESD technologies with unique constraints and characteristics, choosing the best ESD technology for a given application is challenging. Some constraints of the above technologies are listed in Table II.

Our goal is to build a single mathematical model suitable for all ESD technologies. To do so, we first describe our system model in the next section. We summarize the important notations, which will be used in the rest of the paper, in Table I.

III. System model

Energy can be modelled as a continuous-time, fluid stochastic process. That is, at any given time, energy arrival is not a quantized value, unlike Internet packet traffic. Moreover, events in an energy system are not restricted to occur at discrete time instants (except maybe for specific applications). However, we can still assume a discrete-time model (which simplifies analysis) as long as the time granularity is chosen such that the precision is kept above an acceptable threshold. We consider a fluid-flow, but discrete-time model, where time is slotted $t = 0, T_u, 2T_u, \ldots$, with T_u being the time unit. To simplify notation, we drop T_u from our formulation by assuming $T_u = 1$. Generalizing the formulas for any T_u is a matter of additional

notations. We consider a renewable energy source, which is meant to serve a stochastic demand, using an ESD as a backup storage (see Fig. 2) to smooth out demand or source fluctuations. Denote by $S(t)$ and $D(t)$, respectively, the available power from the energy source and the demand power at time t. To simplify notation, we write $D(s,t)$ and $S(s,t)$ to, respectively, mean $\sum_{\tau=s+1}^{t} D(\tau)$ and $\sum_{\tau=s+1}^{t} S(\tau)$ (e.g., $S(t-1,t) = S(t)$).

In our model, renewable energy is preferentially used to serve the demand, i.e., without going through the ESD. If, in a given time slot t, the available renewable power is insufficient (i.e., $S(t) < D(t)$), the energy stored in ESD, if any, can be used to make up the difference. Moreover, if the available renewable power in a time slot t is larger than the demand power (i.e., $S(t) > D(t)$), then the surplus energy ($(S(t) - D(t))T_u$) is stored in the ESD, if it is not yet full. All incoming power exceeding ESD's charging rate limit α_c is dropped. Moreover, the ESD loses a fraction of $1-\eta$ of the total energy being stored in the ESD due to ESD efficiency. The energy stored in the ESD is discarded with rate γ due to ESD self-discharge. The ESD cannot be discharged faster than α_d. Finally, the ESD lifetime constraint is met if only a DoD fraction≤ 1 of the entire ESD is used.

For an ideal ESD (i.e., $\alpha_c, \alpha_d{=}\infty$, $\eta, \text{DoD}{=}1$, $\gamma{=}0$), the complicated ESD model in Fig. 2 reduces to the simple model in Fig. 3, which is identical to a buffer in a network where the input traffic S enters a finite queue of size B with available (time-varying) service rate D. This enables elegant performance analysis of energy systems by adopting standard techniques from the rich literature on performance analysis of teletraffic networks. This is the model that has been used in recent analyses of energy systems [3], [22], [23]. However, ignoring the non-ideal ESD behaviour in the simple model brings into question the validity of these results. Our plan of attack, therefore, is to convert the complex system model of Fig. 2 to an *equivalent* simple model with appropriately modified system parameters (Fig. 4). *This would allow the analytical results that assume ideal ESD behaviour to be suitably transformed to take into account non-ideal ESD behaviour.* We discuss the equivalent model in more detail in Section IV.

IV. Modelling Non-ideal ESDs

In this section, we show how to choose appropriate parameters so that the complex system model of Fig. 2 is converted to the ideal (simple) model of Fig. 4. We begin by noting that the

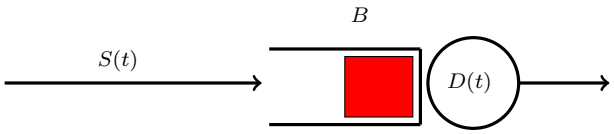

Fig. 3: Equivalent model of Fig. 2, when the ESD is ideal ($\alpha_c, \alpha_d{=}\infty$, η, DoD=1, $\gamma{=}0$).

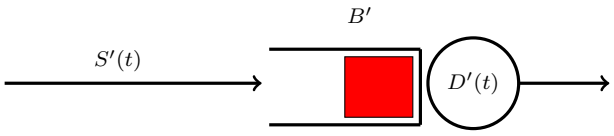

Fig. 4: Converting a non-ideal storage model to an ideal one by defining virtual source S', demand D', and storage size B'.

storage state of charge $b(t)$ in the complex system model (Fig. 2) at any time t is given by

$$b(t) = \min\Big(B \times DoD,\ \Big[b(t-1) + \min\left([S(t) - D(t)]_+, \alpha_c\right)\eta - \min([D(t) - S(t)]_+, \alpha_d) - \gamma\Big]_+\Big), \tag{1}$$

where $[x]_+ = \max\{0, x\}$ for any x. For an ideal ESD (i.e., $\alpha_c, \alpha_d{=}\infty$, η, DoD=1, $\gamma{=}0$), Eq. (1) reduces to

$$b(t) = \min\left(B, [b(t-1) + S(t) - D(t)]_+\right), \tag{2}$$

which is equivalent to the recursive backlog process in teletraffic theory with traffic arrival S, service rate $D(t)$ at any time t, and queue size B [12]. Unfortunately, unlike Eq. (2), Eq. (1) cannot be mapped to a backlog process in teletraffic theory. In the following, we incorporate the storage imperfections, by defining *virtual* power source and demand processes, to simplify the non-ideal storage model.

Lemma 1 (Equivalent simple queue)**.** *Suppose that an intermittent power source S serves a stochastic demand power D. A non-ideal ESD, with size B and parameters α_c, α_d, η, γ and DoD, is used to provide power during a power shortage (i.e., $[D(t) - S(t)]_+$) and also to store the surplus power (i.e., $[S(t) - D(t)]_+$) at any time instant t (Fig. (2)). The state of charge of the ESD in this model is equivalent to that of an ideal ESD model (Fig. 4), where power source S, power demand D, and ESD size B are, respectively, replaced by a virtual source S', a virtual*

demand D', and a virtual ESD size B', given by

$$S'(t) = S(t) - (1-\eta)[S(t) - D(t)]_+ - \eta[S(t) - D(t) - \alpha_c]_+ \tag{3}$$

$$D'(t) = D(t) - [D(t) - S(t) - \alpha_d]_+ + \gamma, \tag{4}$$

$$B' = B \times \textbf{\textit{DoD}}. \tag{5}$$

Proof. We need to show that Eq. (1) can be rewritten as:

$$b(t) = \min\left(B', [b(t-1) + S'(t) - D'(t)]_+\right) \tag{6}$$

which is the equivalent simple system model of Fig. 4. Replacing $B \times DoD$ in Eq. (1) by B' in Eq. (6) follows from the definition of B' in Eq. (5). To study the second term in Eq. (6), we consider two cases:

• **Case 1: (**$S(t) < D(t)$**):** In this case, Eq. (1) reduces to

$$b(t) = \min\left(B', [b(t-1) \underbrace{- \min(D(t) - S(t), \alpha_d) - \gamma}_{:=X_1}]_+\right).$$

With some manipulations, we can rewrite X_1 in the above equation as

$$\begin{aligned} X_1 &= \max(S(t) - D(t), -\alpha_d) - \gamma \\ &= S(t) - D(t) + \max\big(0, D(t) - S(t) - \alpha_d\big) - \gamma \\ &= S'(t) - D'(t), \end{aligned}$$

where in the second line we use $-\min\{x\} = \max\{-x\}$ for any x. The last line is obtained using Eqs. (3)-(4) and considering the case of $S(t) < D(t)$.

• **Case 2: (**$S(t) \geq D(t)$**):** In this case, Eq. (1) reduces to

$$b(t) = \min\left(B', [b(t-1) + \underbrace{\min\left(S(t) - D(t), \alpha_c\right)\eta - \gamma}_{:=X_2}]_+\right).$$

With some manipulations, we can rewrite X_2 in the above equation as

$$\begin{aligned} X_2 &= S(t) - D(t) + \min\big((\eta-1)(S(t)-D(t)), \\ &\qquad\qquad \alpha_c\eta - S(t) + D(t)\big) - \gamma \\ &= S(t) - D(t) - (1-\eta)(S(t)-D(t)) \\ &\qquad - \eta\max(0, S(t)-D(t)-\alpha_c) - \gamma \\ &= S'(t) - D'(t), \end{aligned}$$

where the last line is obtained using Eqs. (3)-(4) and considering the case of $S(t) \geq D(t)$.

□

Remark: The choices of non-negative virtual processes, which convert Fig. 2 to Fig. 4, are not unique. The specific choices we made in Eqs. (3)-(5) greatly facilitate the use of this model in further analysis by separating the impact of imperfections from the original processes. In particular, Eqs. (3)-(4) present the imperfections as additional or subtracting terms to the original source and demand processes.

In the next section, we will employ Lemma 1 to analyze a non-ideal ESD using network calculus [5], [7], [15]. We use this approach because it correctly models the non-asymptotic, non-stationary, and fluid flow aspects of the smart grid. Moreover, it can be used to study a broad range of arrival processes including Makovian, self-similar, and even heavy-tailed processes [16]. The key aspect of network calculus is that it models stochastic processes as bounds on the tail distributions.

V. Using Network Calculus to analyze ESDs

In network calculus, stochastic processes are modelled by *envelopes*, which can be of several types. One of the most widely used ones is called *statistical sample path envelope* [11], defined next. A non-decreasing function $\overline{\mathcal{A}}$ is a statistical sample path *upper* envelope for process A with bounding function $\bar{\varepsilon}$ if it satisfies the following at any time $t \geq 0$ and for any $x \geq 0$

$$\Pr\left\{\max_{s\leq t}\big(A(s,t) - \overline{\mathcal{A}}(t-s)\big) > x\right\} \leq \bar{\varepsilon}(x). \tag{7}$$

Likewise, $\underline{\mathcal{A}}$ is a statistical sample path *lower* envelope for process A with bounding function $\underline{\varepsilon}$ if at any time $t \geq 0$ and for any $x \geq 0$

$$\Pr\left\{\max_{s \leq t} (\underline{\mathcal{A}}(t-s) - A(s,t)) > x\right\} \leq \underline{\varepsilon}(x). \tag{8}$$

Sample path envelopes for a given process can be computed either from measurement traces of that process or from an analytical model of that process (e.g., On-off Markov model). We now describe how to compute sample path envelopes from measurement traces consisting of multiple trajectories A^i indexed by i.

The lower bounding function $\underline{\varepsilon}$ is computed as follows: Construct a set Y with elements $Y^{i,t}$ chosen at time $t \geq 0$ corresponding to a trajectory A^i such that

$$Y^{i,t} = \max_{0 \leq s \leq t} (\underline{\mathcal{A}}(t-s) - A^i(s,t)). \tag{9}$$

Then, from Eq. (8), $\underline{\varepsilon}$ can be chosen to be the CCDF of any distribution that fits Y.

Note that for a given measurement trace, infinitely many models can be proposed by varying $\underline{\mathcal{A}}$ and computing the corresponding bounding function $\underline{\varepsilon}$. Thus, modelling a stochastic process given a measurement trace using this approach consists of three steps: (1) choose an envelope ($\underline{\mathcal{A}}$), (2) characterize the bounding function for the tail bound distribution, and (3) compute the parameters of that distribution.

A similar approach can be used to compute $\overline{\varepsilon}$.

A. Existing performance bounds for ideal ESDs

Two metrics are widely used to characterize energy system performance. *Loss of power* $l(t)$ at time step t occurs if demand is unmet at that time from the sum of renewable power and stored energy. *Waste of power* $w(t)$ at time step t is the amount of power that is wasted in that time slot due to non-ideal ESD behaviour or limited ESD size. The loss of power and waste of power probabilities have been computed in recent work, under the assumption of *ideal* ESD behaviour [3], [22], [23], as follows.

Theorem 1 (Existing performance bounds for ideal ESDs [22])**.** *Consider the same scenario as in Lemma 1 with an ideal ESD. Suppose we are given a statistical sample path lower (upper) envelope* $\underline{\mathcal{S}}$ *(*$\overline{\mathcal{S}}$*) on the intermittent energy source with a bounding function* $\underline{\varepsilon}_s$ *(*$\overline{\varepsilon}_s$*). In addition, assume that there is a statistical sample path upper (lower) envelope* $\overline{\mathcal{D}}$ *(*$\underline{\mathcal{D}}$*) on the demand*

power in the sense of Eq. (7) with a bounding function $\overline{\varepsilon}_d$ ($\underline{\varepsilon}_d$). Then, the loss of power $l(t)$ and the waste of power $w(t)$ at time t, satisfy the following

$$\Pr\{l(t) > 0\} \leq \overline{\varepsilon}_d \otimes \underline{\varepsilon}_s \left(B - \max_{0 \leq \tau \leq t} (\overline{\mathcal{D}}(\tau) - \underline{\mathcal{S}}(\tau)) \right) \tag{10}$$

$$\Pr\{w(t) > x\} \leq \underline{\varepsilon}_d \otimes \overline{\varepsilon}_s \left(B + x - \max_{0 \leq \tau \leq t} (\overline{\mathcal{S}}(\tau) - \underline{\mathcal{D}}(\tau)) \right), \tag{11}$$

where $\otimes$ is the min-plus convolution *operator defined as*

$$f_1 \otimes f_2(u) = \min_{0 \leq s \leq u} (f_1(s) + f_2(u - s)) \tag{12}$$

for any non-negative functions f_1 and f_2 and any constant u.

We will extend this theorem using Lemma 1 to derive performance bounds for non-ideal ESDs in the next section.

B. Performance bounds for non-ideal ESDs

The waste of power in an ideal ESD at time t maps simply to the traffic loss (when an arrival is dropped because the queue is full) in a teletraffic queue of size B, with input traffic $S(t)$, and a service rate $D(t)$ (see Eq. (2)). Thus, the non-recursive backlog formulation from [12] is used to characterize the waste of power in an ideal ESD in [22]

$$w_{ideal}(t) = \min_{0 \leq u < t} \Bigg(\max_{u \leq s < t} \left([S(s,t) - D(s,t) - BI_{t>0}]_+ \right), \\ S(u,t) - D(u,t) + BI_{u>0} - BI_{t>0} \Bigg), \tag{13}$$

where for any expression x, $I_x = 1$ if x is true and $I_x = 0$, otherwise.

The waste of power in an ideal ESD happens only due to limited ESD size. However, the total waste of power in a non-ideal ESD, consists of the power waste due to the storage imperfections $w_{\alpha_c,\gamma,\eta}$ and the waste of power due to finite storage size w_B, i.e.,

$$w_{non-ideal}(t) = w_{\alpha_c,\gamma,\eta}(t) + w_B(t). \tag{14}$$

w_B is characterized by replacing the original processes with the virtual ones (from Lemma 1) in Eq. (13) and $w_{\alpha_c,\gamma,\eta}$ satisfies

$$w_{\alpha_c,\gamma,\eta}(t) \leq S(t) - S'(t) + \gamma, \tag{15}$$

where $S(t) - S'(t)$ accounts for all the power waste occurring due to the ESD charging rate limit (α_c), ESD inefficiency (η), and depth of discharge (DoD). Eq. (15) holds as an inequality, since it assumes that the self-discharge is always γ, meaning that the state of charge is never less than γ.

The loss of power event can be characterized using the concept of the *deficit* state of charge. The deficit state of charge b_d is the energy required to fully charge the ESD and at any time t and is given by

$$b_d(t) = \min(B, [b_d(t-1) + D(t) - S(t)]_+). \tag{16}$$

Importantly, the loss of power event occurs when the ESD state of charge crosses zero or, equivalently, when the deficit state of charge crosses B. Thus, from Eq. (16), the loss of power event is equivalent to the traffic loss in a teletraffic system in a queue with size B, traffic arrival D, and service rate S [22]

$$l_{ideal}(t) = \min_{0 \le u < t} \Bigg(\max_{u \le s < t} \left([D(s,t) - S(s,t) - BI_{t>0}]_+ \right), \\ D(u,t) - S(u,t) + BI_{u>0} - BI_{t>0} \Bigg). \tag{17}$$

The loss of power in an ideal ESD happens only due to an empty ESD. In a non-ideal ESD, however, the loss of power can happen either due to the empty ESD, l_B, or due to the limited discharge rate of ESD, l_{α_d}, which may prevent the entire demand from being met. That is

$$l_{non-ideal}(t) = l_{\alpha_d}(t) + l_B(t). \tag{18}$$

l_B can be computed by simply replacing the original processes with virtual ones in Eq. (17). l_{α_d} is the difference between the power shortage and the discharge rate limit (i.e., $[D(t) - S(t) - \alpha_d]_+$), which (from Eq. (4)) is equivalent to

$$l_{\alpha_d}(t) = [D(t) - S(t) - \alpha_d]_+ = D(t) - D'(t) + \gamma. \tag{19}$$

Using the above definitions, we can compute performance bounds for non-ideal ESDs as:

Theorem 2 (Performance bounds for non-ideal ESDs)**.** *Consider the same scenario as in Lemma 1. S' and D' are, respectively, the virtual source and virtual demand as defined in Lemma 1. Suppose we are given a sample path lower (upper) envelope $\underline{\mathcal{S}}'$ ($\overline{\mathcal{S}}'$) on $S'(t)$ with a bounding function*

$\underline{\varepsilon}'_s$ ($\overline{\varepsilon}'_s$). In addition, suppose we are given a sample path lower (upper) envelope $\underline{\mathcal{D}}'$ ($\overline{\mathcal{D}}'$) on D' with a bounding function $\underline{\varepsilon}'_d$ ($\overline{\varepsilon}'_d$). If for some constant $\underline{\varepsilon}'_0$ and a function $\overline{\varepsilon}'_0$ the following hold at any time $t \geq 0$ and for any $x \geq 0$

$$\Pr\{S'(t) - D'(t) > x\} \leq \overline{\varepsilon}'_0(x) \tag{20}$$

$$\Pr\{D'(t) - S'(t) > 0\} \leq \underline{\varepsilon}'_0 \tag{21}$$

$$\Pr\{S(t) - S'(t) + \gamma > x\} \leq \varepsilon'_w(x), \tag{22}$$

$$\Pr\{D(t) - D'(t) + \gamma > 0\} \leq \varepsilon'_l, \tag{23}$$

then, the loss of power and the waste of power at time t satisfy the following:

$$\Pr\{l(t) > 0\} \leq \varepsilon'_l + \min\Bigg(\underline{\varepsilon}'_0, \overline{\varepsilon}'_d \otimes \underline{\varepsilon}'_s \left(B' - \max_{0\leq\tau\leq t}(\overline{\mathcal{D}}'(\tau) - \underline{\mathcal{S}}'(\tau))\right)\Bigg) \tag{24}$$

$$\Pr\{w(t) > x\} \leq \min\Bigg(\varepsilon'_w \otimes \overline{\varepsilon}'_0(x), \varepsilon'_w \otimes \left(\underline{\varepsilon}'_d \otimes \overline{\varepsilon}'_s\big(B' + x - \max_{0\leq\tau\leq t}(\overline{\mathcal{S}}'(\tau) - \underline{\mathcal{D}}'(\tau))\big)\right)\Bigg). \tag{25}$$

Proof. We prove the waste of power bound (Eq. (13)) in the following. The proof of the loss of power bound is less complicated and follows similar steps using Eqs. (17-19).

Combining Eqs. (14)-(15)-(22) and using the fact that $\Pr(A + B > a + b) \leq \Pr(A > a) + \Pr(B > b)$ for any random variables A and B and constants a and b, we have

$$\begin{aligned}\Pr\{w(t) > x\} &\leq \min_{0\leq x_B\leq x}\big(\Pr\{w_{\alpha_c,\gamma,\eta}(t) > x - x_B\} \\ &\qquad + \Pr\{w_B(t) > x_B\}\big) \\ &\leq \min_{0\leq x_B\leq x}\big(\varepsilon_w(x - x_B) + \Pr\{w_B(t) > x_B\}\big)\end{aligned} \tag{26}$$

$w_B(t)$ is given by replacing the original processes with the virtual ones in Eq. (13). An upper bound on the resulting equation can be obtained by choosing two specific values for u ($= t - 1$

and $= 0$) in the minimization in Eq. (13), i.e., for any $t > 1$

$$w_B(t) \leq \min\Big([S'(t) - D'(t)]_+, \max_{0\leq\tau<t}\left([S'(\tau,t) - D'(\tau,t) - B']_+\right)\Big). \tag{27}$$

In addition, we have the following upper bound on the second term in Eq. (27)

$$\begin{aligned}
&\max_{0\leq\tau<t}\left(S'(\tau,t) - D'(\tau,t) - B'\right)\\
&\quad\leq \underbrace{\max_{0\leq\tau<t}\left(S'(\tau,t) - \overline{\mathcal{S}}'(t-\tau)\right)}_{:=U}\\
&\qquad + \underbrace{\max_{0\leq\tau<t}\left(\underline{\mathcal{D}}'(t-\tau) - D'(\tau,t)\right)}_{:=V}\\
&\qquad + \underbrace{\max_{0\leq\tau<t}\left(\overline{\mathcal{S}}'(\tau) - \underline{\mathcal{D}}'(\tau)\right) - B'}_{:=-Z}.
\end{aligned} \tag{28}$$

Using the above inequalities, we can write

$$\begin{aligned}
&\Pr\{w_B(t) > x_B\}\\
&\leq \Pr\Bigg\{\min\Bigg([S'(t) - D'(t)]_+,\\
&\qquad \max_{0\leq\tau<t}\left([S'(\tau,t) - D'(\tau,t) - B]_+\right)\Bigg) > x_B\Bigg\} &(29)\\
&\leq \min\Bigg(\Pr\left\{S'(t) - D'(t) > x_B\right\},\\
&\qquad \Pr\left\{\max_{0\leq\tau<t}(S'(\tau,t) - D'(\tau,t) - B) > x_B\right\}\Bigg) &(30)\\
&\leq \min\left(\overline{\varepsilon}'_0(x_B), \min_{z_1+z_2=Z+x_B}\left(\Pr\{U > z_1\} + \Pr\{V > z_2\}\right)\right) &(31)\\
&\leq \min\left(\overline{\varepsilon}'_0(x_B), \underline{\varepsilon}'_d \otimes \overline{\varepsilon}'_s\left(B' + x_B - \max_{0\leq\tau\leq t}(\overline{\mathcal{S}}'(\tau) - \underline{\mathcal{D}}'(\tau))\right)\right) &(32)
\end{aligned}$$

where we use Eq. (27) in the second line. Eq. (30) is an upper bound on Eq. (29) using the fact that $P(A \cap B) \leq \min(P(A), P(B))$ for any events A and B. We also dropped $[.]_+$ since $x_B \geq 0$. Eq. (31) uses Eq. (20) to obtain the first term in the minimization and uses Eq. (28)

and the fact that $\Pr(A+B>a+b) \leq \Pr(A>a)+\Pr(B>b)$ for any random variables A and B and constants a and b. The last line uses the definition of min-plus convolution from Eq. (12) and the assumption that $\underline{\mathcal{D}}'$ and $\overline{\mathcal{S}}'$ are, respectively, a lower bound on D' and an upper bound on $S'(t)$ with bounding functions $\underline{\varepsilon}'_d$ and $\overline{\varepsilon}'_s$.

Combining Eq. (26) and Eq. (32) and the convolution definition in Eq. (12) proves the theorem. □

Remark: Besides allowing the computation of performance bounds for non-ideal ESDs, our work also improves on the known results for the case of ideal ESDs in Theorem 1; it provides tighter bounds because the first terms in the minimization in two bounds of Eqs. (24)-(25) (i.e., $\underline{\varepsilon}'_0$ and $\varepsilon'_w \otimes \overline{\varepsilon}'_0(x)$) were not considered in [22]. These terms affect performance greatly when the ESD size is small. In particular, for the case of an energy system with no storage, Theorem 1 says that the probabilities of loss of power and waste of power are upper bounded by 1, whereas our theorem returns non-trivial bounds.

The performance bounds found in Theorem 2 hold for general sample path envelopes and bounding functions. In the next section, we compute bounds for the case where the source and demand processes have simple exponential tail bounds.

C. Computing bounds for exponential tail bounds

It has been shown, in the literature of network calculus, that even simple functions can characterize several complex stochastic processes. In fact, the trivial function $\mathcal{A}(t) = rt$ as a sample path envelope and an exponential decay rate $ae^{-\xi t}$ as a tail bound can characterize a large class of processes called exponentially bounded burstiness processes (EBB) [25], which includes Markov modulated processes. In our work, we model a more general class of processes than EBB by using affine functions of the form $\mathcal{A}(t) = [a \pm rt]_+$ as envelopes with exponential decay rates as bounding functions. Specifically,

$$\underline{\mathcal{S}}'(t) = [\rho_1 t - \sigma_1]_+; \qquad \underline{\varepsilon}'_s(x) = p_1 e^{-\beta_1 x} \tag{33}$$

$$\overline{\mathcal{S}}'(t) = \rho_2 t + \sigma_2; \qquad \overline{\varepsilon}'_s(x) = p_2 e^{-\beta_2 x} \tag{34}$$

$$\underline{\mathcal{D}}'(t) = [\rho_3 t - \sigma_3]_+; \qquad \underline{\varepsilon}'_d(x) = p_3 e^{-\beta_3 x} \tag{35}$$

$$\overline{\mathcal{D}}'(t) = \rho_4 t + \sigma_4; \qquad \overline{\varepsilon}'_d(x) = p_4 e^{-\beta_4 x} \tag{36}$$

for some ρ_j, σ_j, p_j, β_j, $(1 \leq j \leq 4)$. In addition to our assumptions on the choices of envelopes, we also assume

$$\overline{\varepsilon}'_0(x) = p_5 e^{-\beta_5 x}; \qquad \varepsilon'_w(x) = p_6 e^{-\beta_6 x}; \tag{37}$$

for some p_5, p_6, β_5, β_6. Inserting the above choices in Theorem 2, we can compute performance bounds for energy systems with non-ideal ESDs.

Recall that the bounds in Theorem 2 use the convolution operation, and each convolution is a minimization over a free parameter (see Eq. (12)). Computing this minimum is challenging for general functions. Although, for the case of exponential distributions, one can use Lemma 3 from [10] to compute these convolutions, we decided to compute simpler suboptimal, albeit good, values for the free parameter in the convolution operation by choosing identical exponents in the convolving functions. With this simplification, and if, respectively, $\rho_1 \geq \rho_4$ and $\rho_3 \geq \rho_2$ (a stability condition), we get

$$\begin{aligned} \Pr\{l(t) > 0\} &\leq \varepsilon'_l \\ &+ \min\left(\underline{\varepsilon}'_0, (p_1 + p_4) e^{\left\{-\frac{\beta_1\beta_4}{\beta_1+\beta_4}(B-\sigma_1-\sigma_4)\right\}}\right) \end{aligned} \tag{38}$$

and

$$\begin{aligned} \Pr\{w(t) > x\} \leq \min\Bigg(& (p_6 + p_5) e^{-\frac{\beta_5\beta_6 x}{\beta_5+\beta_6}}, \\ & \left(p_6 + (p_2 + p_3) e^{\left\{-\frac{\beta_2\beta_3}{\beta_2+\beta_3}(B-\sigma_2-\sigma_3)\right\}}\right) e^{-\beta_w x}\Bigg), \end{aligned} \tag{39}$$

where $\beta_w = (1/\beta_2 + 1/\beta_3 + 1/\beta_6)^{-1}$.

D. Steps to evaluate bounds for a measurement trace

We now describe the steps necessary to compute bounds on loss of power probability and waste of power probability using our approach. Recall that we are given measurement traces for S and D and also the physical characterizations of the ESD.

First, compute the virtual source S', demand D', and ESD size B' using Lemma 1. Second, compute the rates in the sample path envelopes (i.e., ρ_j in Eqs. (33-36)) by setting ρ_j $(\forall j)$ to the long-term average power of its corresponding process (e.g., $\rho_1 = \frac{\sum_{t=1}^{T} S'(t)}{T}$, where T is the time length of the measurement trace.). Third, verify that the stability condition is met. That is,

check that $\rho_1 \geq \rho_4$ and $\rho_3 \geq \rho_2$, which otherwise and respectively, lead to the loss of power probability and the waste of power probability to be trivially bounded by 1. Fourth, compute the four bounding functions, with parameters p_j and β_j, treating σ_js as free parameters, as follows: For a fixed σ_j, construct the set Y (see Eq. (9)) for the corresponding virtual process and envelope (e.g. $\overline{\mathcal{S}}'$). Note that the elements of Y must be non-negative. Thus, set all negative elements of Y to zero. To avoid the bias of the zero elements in the fitted distribution, set p_j to the ratio of the non-zero elements of Y to the total number of elements. Then, β_j is the parameter of the exponential decay that is fitted to the non-zero elements of Y. Fifth, use similar steps to compute p_5, p_6, β_5, and β_6. Finally, by turning Eqs. (33-36) to functions of the free parameter σ_j, minimize them over that parameter to find the optimal value of σ_j.

E. Limitations

Although our work incorporates many important ESD imperfections, it does not model *all* ESD imperfections. To begin with, the impact of temperature on the ESD operation is as yet unknown, and therefore has not been incorporated into our model. Second, we do not consider the dependence of the ESD charging rate limit on the ESD state of charge because this dependence has not yet been adequately quantified. Third, ESD self-discharge rate can decay non-linearly as a function of time for some technologies (e.g., exponential decay rate for Scaps), whereas, for simplicity, we assume a linear function of time. Finally, we do not model the fact that ESD capacity gradually decays over time. Fortunately, this does not affect our analysis, because the decay rate is much slower than the ESD charge/discharge processes. We anticipate that, as ESD behaviour is better quantified in the future, our models can be adapted to include these other non-ideal behaviours, as appropriate.

VI. Evaluation

In this section, we validate our analysis using the widely used wind turbine power traces from the US West Coast, with a 10-minute time resolution ($T_u = 10$min), freely available from NREL [2].

We assume that this wind power is used to serve a constant demand of 0.1MW for loss of power. For evaluating the waste of power, we use a higher demand of 0.5MW with an ESD of size 10MWh, to keep the magnitude of the waste of power numerically manageable.

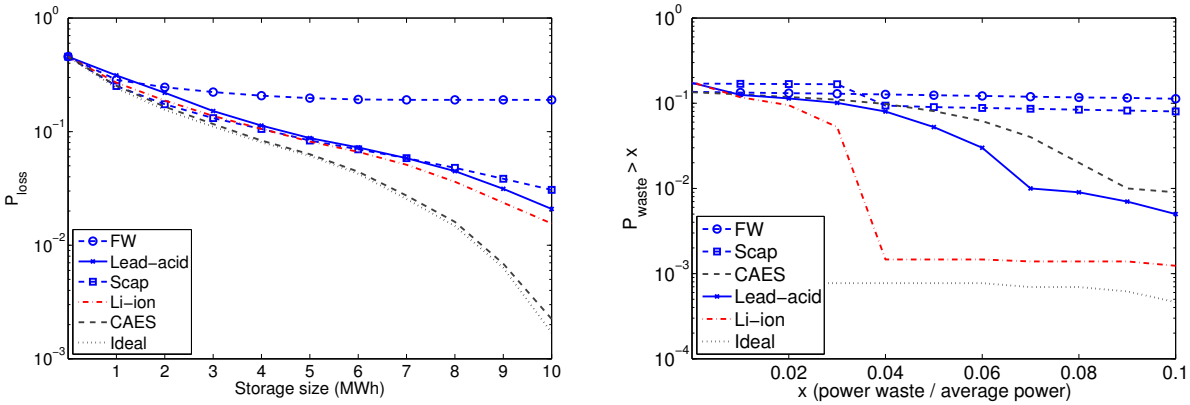

(a) Loss of power probability ($D(t)$=0.1MW)

(b) Waste of power probability ($D(t)$=0.5MW and B=10MWh)

Fig. 5: The impact of ESD imperfections on P_{loss} and P_{waste} for different ESD technologies.

We compare the performance of the five ESD technologies in Section II: lithium-ion battery, supercapacitor (Scap), lead-acid battery, flywheel (FW), and compressed-air energy storage (CAES). The physical constraints of these technologies are as in Table II.

A. The impact of imperfections

In this section, we use numerical simulations to investigate the impact of ESD imperfections on energy system performance. For each ESD technology, we compute the actual loss of power and the waste of power probabilities by simulating the ESD state of charge process, using Eq. (1), and computing the quantiles (i.e., CCDF) of the performance metrics. We also show the performance metrics of an ideal ESD to study the impact of imperfections for each ESD technology.

Fig. 5a shows the loss of power probability as a function of ESD size for each ESD technology. This graph demonstrates the substantial impact of the physical constraints; non-ideal ESDs have significantly different loss of power probabilities compared to an ideal ESD for the same storage size. This vividly demonstrates the need for the analytical modelling of ESD imperfections, especially for larger storage sizes. This figure also shows the dramatic difference in behaviour across ESD technologies, again, especially for larger storage sizes. For instance, with a storage size of 10MWh, an ideal ESD or a CAES ESD would have a loss of power probability of only

0.002, but a flywheel would have a loss of power probability of as much as 0.2, two orders of magnitude greater. We attribute this to the high self-discharge rate of a flywheel, which is not modelled by the existing analytical models.

Fig. 5a also highlights a very interesting fact: Scaps outperform lithium-ion batteries for small ESD sizes, but are outperformed by lithium-ion batteries as the storage size increases beyond a certain threshold. This is due to the fact that the main physical constraints of lithium-ion batteries are their charging rate limits and DoD, which will be less pronounced as the storage size increases (since the charging rate limit is proportional to the storage size for batteries and DoD has a smaller impact in large storage sizes). In contrast, the main physical constraint of Scaps is their large discharge rate, which is more pronounced as the storage size increases. This is due to the fact that as the ESD size increases, the average amount of the stored energy in the ESD increases, which in turn, leads to larger waste of power due to self-discharge. Again, this crossover point in performance is not modelled by the ideal ESD model.

Fig. 5b shows the tail bound distribution of the waste of power probability for the five ESD technologies along with that of an ideal ESD. This graph also corroborates the fact that ignoring the physical constraints of ESDs drastically underestimates the required resources for all technologies and that the ESD technology highly impacts the waste of power.

B. Accuracy of analytical performance bounds

Section VI-A computed performance bounds through numerical simulations. Here, we evaluate the quality of our analytical bounds from Theorem 2 in Fig. 6. Though not shown here due to lack of space, we first used QQ-plots to verify that simple exponential decay functions do adequately characterize the stochastic wind power process. This allows us to use Eqs. (38)-(39) as performance bounds and to compare the numerical and analytical performance bounds of three selected ESD technologies.

Fig. 6a compares the loss of power probability and Fig. 6b the waste of power probability. Our analytical bounds closely match numerical simulations, especially for loss of power probabilities. This demonstrates the usefulness of our analytical approach.

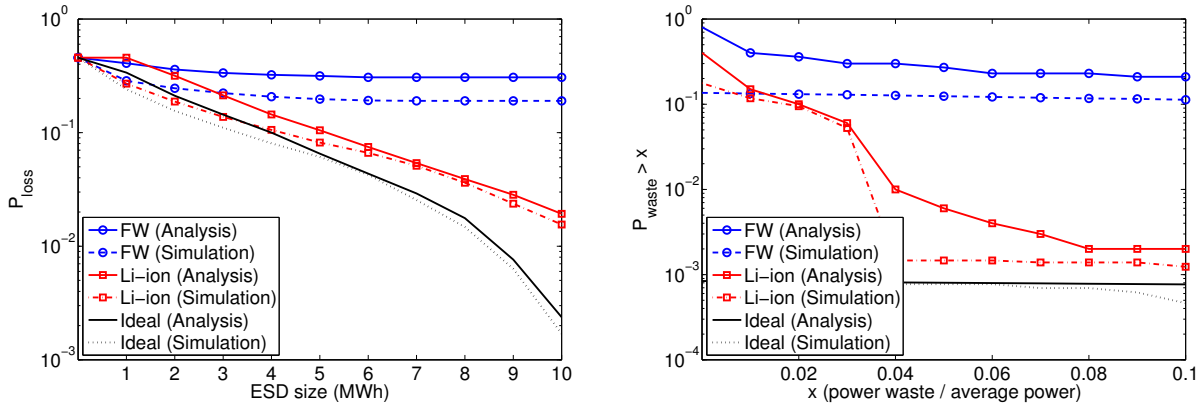

(a) Loss of power probability ($D(t)$=0.1MW)

(b) Waste of power probability ($D(t)$=0.5MW and B=10MWh)

Fig. 6: Evaluating the accuracy of our analysis: the analytical performance bounds are reasonably tight upper bounds on numerically obtained values.

VII. Conclusion

By smoothing out variations in the supply and demand processes, energy storage devices (ESDs) are likely to play a significant role in all future energy systems. Sizing and choosing the best ESD technology is a critical task, that is usually accomplished using extensive simulations. Apart from time complexity, dimensioning through simulation requires large datasets which are often difficult to obtain.

An analytical approach, in contrast, requires smaller datasets and allows great flexibility in choosing design parameters. In recent work, an elegant mapping between smart grids and queuing systems in teletraffic theory has enabled the performance analysis of energy systems drawing on a large and sophisticated literature in this area [3], [22], [23]. A critical issue is that an analytical model should model non-ideal ESD behaviour, rather than assuming them to be identical to memory buffers in the Internet, as is the case in current work.

Our first main result is that by defining virtual source and demand processes, we can use teletraffic analysis even for a non-ideal ESD. Our second main result is to extend prior work using stochastic network calculus to compute upper bounds on the loss of power and waste of power probabilities for non-ideal ESDs. Using numerical simulations over a large dataset of wind

power, we show that (1) the storage imperfections have a significant impact on the performance of energy systems, and (2) our analytical bounds for non-ideal ESDs are quite tight.

Our work is important in that it provides a *general* framework to analyze stochastic energy systems with *any* non-ideal ESD technology. Yet, we recognize that it does not model some classes of ESD imperfections that are still poorly understood in the literature. In future work, we anticipate incorporating these into our general non-ideal ESD model.

REFERENCES

[1] http://batteryuniversity.com.

[2] http://wind.nrel.gov/Webnrel/.

[3] O. Ardakanian, S. Keshav, and C. Rosenberg. On the use of teletraffic theory in power distribution systems. In *Proc. of the 3rd International Conference on Future Energy Systems: Where Energy, Computing and Communication Meet*, pages 1 – 10. ACM, 2012.

[4] O. Ardakanian, C. Rosenberg, and S. Keshav. On the impact of storage in residential power distribution systems. *SIGMETRICS Performance Evaluation Review*, 40(3):43 – 47, December 2012.

[5] J. Y. Le Boudec and P. Thiran. *Network Calculus*. Springer Verlag, Lecture Notes in Computer Science, LNCS 2050, 2001.

[6] D. W. H. Cai, S. Adlakha, and K. M. Chandy. Optimal contract for wind power in day-ahead electricity markets. In *Porc. of CDC-ECC*, pages 1521 – 1527, 2011.

[7] C. S. Chang. *Performance guarantees in communication networks*. Springer Verlag, 2000.

[8] M. Chen and G. A. Rincon-Mora. Accurate electrical battery model capable of predicting runtime and I-V performance. *Energy Conversion, IEEE Transactions on*, 21(2):504 – 511, 2006.

[9] C. Chiasserini and R. R. Rao. Energy efficient battery management. *IEEE Journal on Selected Areas in Communications*, 19(7):1235 – 1245, 2001.

[10] F. Ciucu, A. Burchard, and J. Liebeherr. Scaling properties of statistical end-to-end bounds in the network calculus. *IEEE Transactions on Information Theory*, 52(6):2300 – 2312, June 2006.

[11] F. Ciucu and J. Schmitt. Perspectives on network calculus: no free lunch, but still good value. In *Proc. of ACM SIGCOMM Computer Communication Review*, pages 311 – 322, August 2012.

[12] R. L. Cruz and H. N. Liu. Single server queues with loss: A formulation. In *Proc. of CISS*, March 1993.

[13] P. Denholm, E. Ela, B. Kirby, and Michael Milligan. The role of energy storage with renewable electricity generation. Technical Report TP-6A2-47187, NREL, January 2010.

[14] H. He, R. Xiong, and J. Fan. Evaluation of lithium-ion battery equivalent circuit models for state of charge estimation by an experimental approach. *Energies*, 4(4):582 – 598, 2011.

[15] Y. Jiang and Y. Liu. *Stochastic Network Calculus*. Springer Verlag, 2008.

[16] J. Liebeherr, A. Burchard, and F. Ciucu. Non-asymptotic delay bounds for networks with heavy-tailed traffic. In *Proc. of IEEE INFOCOM*, pages 1 – 9, March 2010.

[17] D. Linden and T. B. Reddy. *Handbook of Batteries*. McGraw Hill, 2002.

[18] J. R. Miller. Development of equivalent circuit models for batteries and electrochemical capacitors. In *Proc. of the Fourteenth Annual Battery Conference on Applications and Advances, 1999*, pages 107 – 109, 1999.

[19] A. K. Sinhaa and P. Bajpai. Swarm intelligence based optimal sizing of solar pv, fuel cell and battery hybrid system. In *Proc. of International Conference on Power and Energy Systems Lecture Notes in Information Technology*, pages 467 – 473, October 2012.

[20] A. R. Sparacino, G. F. Reed, R. J. Kerestes, B. M. Grainger, and Z. T. Smith. Survey of battery energy storage systems and modeling techniques. In *Proc. of IEEE Power and Energy Society General Meeting*, pages 1 – 8, 2012.

[21] D. Wang, C. Ren, A. Sivasubramaniam, B. Urgaonkar, and H. Fathy. Energy storage in datacenters: what, where, and how much? In *Proc. of ACM SIGMETRICS/PERFORMANCE*, pages 187–198, June 2012.

[22] K. Wang, F. Ciucu, C. Lin, and S. H. Low. A stochastic power network calculus for integrating renewable energy sources into the power grid. *IEEE Journal on Selected Areas in Communications*, 30(6):1037 – 1048, July 2012.

[23] K. Wu, Y. Jiang, and D. Marinakis. A stochastic calculus for network systems with renewable energy sources. *arXiv:1108.1554v1*, 2011.

[24] H. Yang, L. Lu, and W. Zhou. A novel optimization sizing model for hybrid solar-wind power generation system. *Solar Energy*, 81(1):76 – 84, 2007.

[25] O. Yaron and M. Sidi. Performance and stability of communication networks via robust exponential bounds. *IEEE/ACM Transactions on Networking*, 1(3):372 – 385, June 1993.